$$\tilde{G}_{\phi z}^{HJ^{(i)}}(\rho, n, k_z) = \frac{1}{D_n}\left(\alpha - \frac{\gamma_1}{\gamma_2}\Delta_2\right)M^{(i)} - \epsilon_{eff}(\epsilon_r - 1)\frac{n^2 k_0^2}{a\rho D_n \gamma_1^2 \gamma_2^2} N^{(i)},$$

$$\tilde{G}_{\phi z}^{EJ^{(i)}}(\rho, n, k_z) = j\frac{\eta n\sqrt{\epsilon_{eff}}}{\rho\gamma_1\epsilon_0 D_n}\left(\alpha - \frac{\gamma_1}{\gamma_2}\Delta_2\right)P^{(i)} - j\sqrt{\epsilon_{eff}}(\epsilon_r - 1)\frac{\eta n k_0^2}{aD_n\gamma_1\gamma_2^2} Q^{(i)},$$

$$\tilde{G}_{\rho z}^{HJ^{(i)}}(\rho, n, k_z) = \frac{-n}{\rho\gamma_1 D_n}\left(\alpha - \frac{\gamma_1}{\gamma_2}\Delta_2\right)P^{(i)} + j\frac{n\epsilon_{eff}(\epsilon_r - 1)}{aD_n\gamma_1\gamma_2^2} Q^{(i)}$$

with

$$\eta = \sqrt{\mu_0/\epsilon_0}, \qquad \alpha = \frac{J_n'(\gamma_1 a)}{J_n(\gamma_1 a)},$$

$$X_1 = \frac{H_n^{(1)}(\gamma_2 a)}{J_n(\gamma_2 a)}, \qquad Y_1 = \frac{H_n^{(1)'}(\gamma_2 a)}{J_n'(\gamma_2 a)},$$

$$X_2 = \frac{H_n^{(1)}(\gamma_2 b)}{J_n(\gamma_2 b)}, \qquad Y_2 = \frac{H_n^{(1)'}(\gamma_2 b)}{J_n'(\gamma_2 b)},$$

$$X_3 = \frac{H_n^{(1)}(\gamma_2 \rho)}{J_n(\gamma_2 \rho)}, \qquad Y_3 = \frac{H_n^{(1)'}(\gamma_2 \rho)}{J_n'(\gamma_2 \rho)},$$

$$\gamma_1 = k_0^2 - k_z^2, \qquad \gamma_2 = \epsilon_r k_0^2 - k_z^2,$$

$$M^{(1)} = Q^{(1)} = \frac{J_n'(\gamma_1\rho)}{J_n(\gamma_1 a)}, \qquad N^{(1)} = P^{(1)} = \frac{J_n(\gamma_1\rho)}{J_n(\gamma_1 a)},$$

$$M^{(2)} = \frac{\gamma_1}{\gamma_2}\frac{Y_3 - X_2}{X_1 - X_2}\frac{J_n'(\gamma_2\rho)}{J_n(\gamma_2 a)},$$

$$N^{(2)} = \left(\frac{\gamma_1}{\gamma_2}\right)^2\frac{X_3 - Y_2}{X_1 - Y_2}\frac{J_n(\gamma_2\rho)}{J_n(\gamma_2 a)},$$

$$P^{(2)} = \left(\frac{\gamma_1}{\gamma_2}\right)^2\frac{X_3 - X_2}{X_1 - X_2}\frac{J_n(\gamma_2\rho)}{J_n(\gamma_2 a)},$$

$$Q^{(2)} = \frac{\gamma_1}{\gamma_2}\frac{Y_3 - Y_2}{X_1 - Y_2}\frac{J_n'(\gamma_2\rho)}{J_n(\gamma_2 a)},$$

$$D_n = \epsilon_0\left[\frac{nk_0k_e(\epsilon_r - 1)}{a\gamma_1\gamma_2^2}\right]^2 - \left(\alpha - \frac{\gamma_1}{\gamma_2}\Delta_2\right)\left(\alpha - \frac{\gamma_1}{\gamma_2}\epsilon_r\Delta_1\right),$$

$$\Delta_1 = \frac{H_n^{(1)}(\gamma_2 b)J_n'(\gamma_2 a) - J_n(\gamma_2 b)H_n^{(1)'}(\gamma_2 a)}{H_n^{(1)}(\gamma_2 b)J_n(\gamma_2 a) - J_n(\gamma_2 b)H_n^{(1)}(\gamma_2 a)},$$

$$\Delta_2 = \frac{H_n^{(1)'}(\gamma_2 b)J_n'(\gamma_2 a) - J_n'(\gamma_2 b)H_n^{(1)'}(\gamma_2 a)}{H_n^{(1)'}(\gamma_2 b)J_n(\gamma_2 a) - J_n'(\gamma_2 b)H_n^{(1)}(\gamma_2 a)}.$$

It is also noted that Δ_1 and Δ_2 are calculated using a similar algorithm given in [2], and $J_n(x)$ is a Bessel function of the first kind with order n; $H_n^{(1)}(x)$ is a Hankel function of the first kind with order n. The prime in the equation denotes a derivative with respect to the argument.

References

[1] K. L. Wong and Y. C. Chen, "Resonant frequency of a slot-coupled cylindrical-rectangular microstrip structure," *Microwave Opt. Technol. Lett.*, vol. 7, pp. 566–570, Aug. 20, 1994.

[2] N. G. Alexopoulos and A. Nakatani, "Cylindrical substrate microstrip line characterization," *IEEE Trans. Microwave Theory Tech.*, vol. 35, pp. 843–849, Sept. 1987.

[3] K. L. Wong, Y. T. Cheng, and J. S. Row, "Resonance in a superstrate-loaded cylindrical-rectangular microstrip structure," *IEEE Trans. Microwave Theory Tech.*, vol. 41, pp. 814–819, May 1993.

[4] J. R. Brews, "Characteristic impedance of microstrip lines," *IEEE Trans. Microwave Theory Tech.*, vol. 35, pp. 30–34, Jan. 1987.

Attenuation of the Parasitic Modes in a Shielded Microstrip Line by Coating Resistive Films on the Substrate

Young-Hoang Chou and Shyh-Jong Chung

***Abstract*—In this paper, propagation characteristics of even-symmetric hybrid modes in a waveguide-shielded microstrip line with the presence of the resistive films affixed to the two sides of the center strip is investigated. The method of lines with modifications concerning the inhomogeneity of the surface between the air and substrate layers is used for analysis. After a validity check of the analysis by considering two special structures, i.e., a microstrip line ($R_m = \infty$) and a coplanar waveguide (R_m =0), the resistance R_m and the width W_m of the film are varied to see the influence on the propagation and attenuation constants of the dominant mode as well as the higher-order (parasitic) modes. Optimal combinations of the resistance and the width are found so that the resistive film has the largest attenuating effect on the higher-order modes but has no interference with the dominant one.**

I. Introduction

Microstrip circuits are often enclosed in metal packages to prevent mechanical damage and electromagnetic interferences from the environment and to provide electrical isolation between different parts of the circuits. However, these metal enclosures may have two important influences on the circuit performances. The first is the proximity effect which occurs when the package wall is close to the circuit. The second is the coupling between the circuit signals and the parasitic modes of the housing introduced when the operating frequency is above the cutoff frequency for higher order mode propagation [1], [2]. Proximity effect on the characteristic of the dominant mode can be minimized by the use of an eletrically large enclosure which, however, can support several propagation (parasitic) modes. As indicated in [1], the erratic circuit behaviors caused by the parasitic coupling of these higher-order modes are more important than the proximity effects. Therefore, it is more desirable to device efficient ways to suppress the propagation of these modes.

Several possible approaches for suppressing the parasitic modes were summarized in [3], which included the deformation of the

Manuscript received March 2, 1994; revised Dec. 23, 1994. This work was supported by the National Science Council of the Republic of China Grant NSC 82-0404-E-009-336.

The authors are with the Institute of Communication Engineering, National Chiao Tung University, Hsinchu, Taiwan, R.O.C.

IEEE Log Number 9412061.

0018–9480/95$04.00 © 1995 IEEE

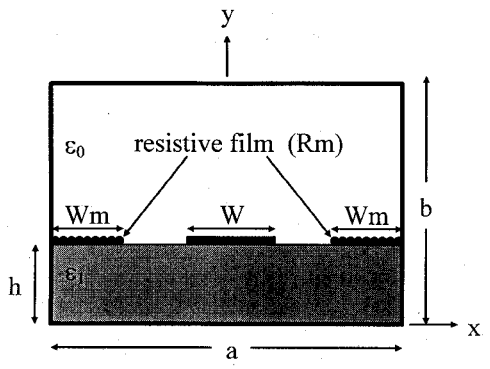

Fig. 1. A waveguide-shielded microstrip line with resistive films coated at the two sides of the center strip. The microstrip and the resistive films are assumed to be of infinitesimal thicknesses.

enclosure to increase the cutoff frequencies of the higher-order modes and the placement of absorbing materials to attenuate the powers of the modes. Armstrong and Cooper [4] experimentally investigated the damping of the package resonant modes by using microwave absorbing materials. Schneider and Glance [5] made an experimental study on the suppression effect of resistive films with respect to the undesired waveguide modes of the suspended microstrip lines. Recently, theoretical analysis have been done by several authors [6]–[8], in which Williams [6] considered the use of the resistive film coated on a dielectric layer which was, in turn, fixed under the lid of a package containing a large MMIC. In his investigation the influence of the circuited bottom substrate was neglected. Chung and Wu [8] analyzed the attenuation effects on the higher-order propagation modes of a resistively coated upper dielectric layer in a waveguide-shielded microstrip line. For the specific housings considered, they predicted a maximum attenuation of 6 dB/cm could be obtained with appropriate film resistance.

In this paper we tackle a similar study with that of [8] but with the resistive films placed at the two sides of the center microstrip. The films can be generated by evaporating or sputtering suitable materials (e.g., NiCr or Ta) on a dielectric substrate or by doping impurities into a semiconductor substrate, both in the process of implementing the microstrip circuit [3]. Since the resistance of the film is proportional to the inverses of the film conductivity and thickness [9], a large range of the resistances can be obtained by controlling these two factors.

II. Formulation

Fig. 1 illustrates a cross-sectional view of the shielded microstrip line to be analyzed, where the strip conductor and the resistive films are assumed to be of infinitesimal thicknesses and are affixed so that the whole structure is symmetric in the x direction. For simplicity, and for the sake that the first higher-order mode for the structure considered is an even one, only the characteristics of even modes are considered.

Following the procedures of the method of lines described in [10], a system equation in the spatial domain is derived

$$\mathbf{Z}(\gamma)\mathbf{J} = \mathbf{E} \tag{1}$$

where the system matrix $\mathbf{Z}$ is a function of the complex propagation constant γ for the mode to be calculated, $\mathbf{J} = \eta_0\ [j\mathbf{J_x^t}, \mathbf{J_z^t}]^\mathbf{t}$, and $\mathbf{E} = [\mathbf{E_x^t}, -\mathbf{jE_z^t}]^\mathbf{t}$ are vectors containing the current and the tangential electric field, respectively, on the interface between the air and the substrate.

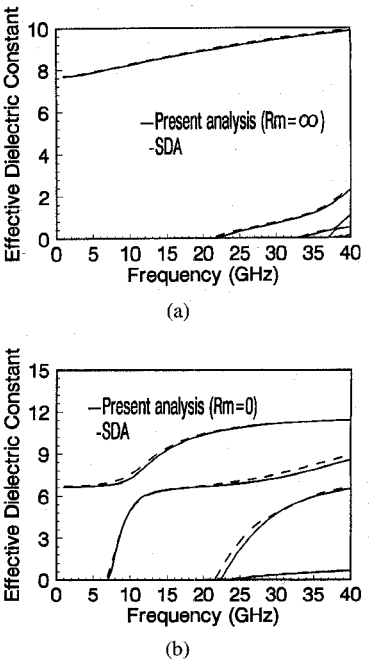

Fig. 2. Dispersion characteristics of (a) a shielded microstrip line ($W = lh$, $R_m = \inf$) and (b) a shielded coplanar waveguide ($W = 1h, W_m = 4.376h$).

After considering the facts that the current and the field vanish, respectively, in the slot and the microstrip regions, a reduced equation according to (1) is derived

$$\mathbf{Z^r}(\gamma)\begin{bmatrix}\mathbf{J_c}\\ \mathbf{J_m}\end{bmatrix} = \begin{bmatrix}0\\ \mathbf{E_m}\end{bmatrix} \tag{2}$$

where $\mathbf{J_c}$ and $\mathbf{J_m}$ are the currents on the strip conductor and the resistive film, and $\mathbf{E_m}$ is the tangential electric field on the film. Now the resistive boundary condition [9] is introduced

$$\mathbf{E_m} = \frac{R_m}{j\eta_0}\mathbf{J_m} \tag{3}$$

with R_m being the resistance of the film. Incorporating this equation into (2) and moving the right-hand side of the resultant equation to the left-hand side, one obtains

$$\mathbf{Z^m}(\gamma)\begin{bmatrix}\mathbf{J_c}\\ \mathbf{J_m}\end{bmatrix} = 0 \tag{4}$$

with

$$\mathbf{Z^m}(\gamma) = \mathbf{Z^r}(\gamma) - \begin{bmatrix}0 & 0\\ 0 & \frac{R_m}{j\eta_0}\end{bmatrix}. \tag{5}$$

The complex propagation constant can then be obtained by enforcing the condition of $\det\{\mathbf{Z^m}(\gamma)\} = \mathbf{0}$.

III. Results and Discussion

In this section some of the numerical results are presented and discussed. The width W of the strip and the thickness h of the substrate both are set to be equal to 0.635 mm. $\epsilon_1 = 11.8\epsilon_0$. The housing of the structure is chosen as $(a \times b =)\ 10h \times 7h$.

As a validity check of the present analysis, we consider two extreme examples of the structure, i.e., a shielded microstrip line and a shielded coplanar waveguide. The former is obtained by setting the film resistance R_m to be infinity. (Note that the resistive film vanishes when $R_m = \infty$.) The latter is gotten when $R_m = 0$ (which makes the resistive film turn to be a perfect electric conductor). Fig. 2(a) shows the dispersion characteristics of the first few modes for the

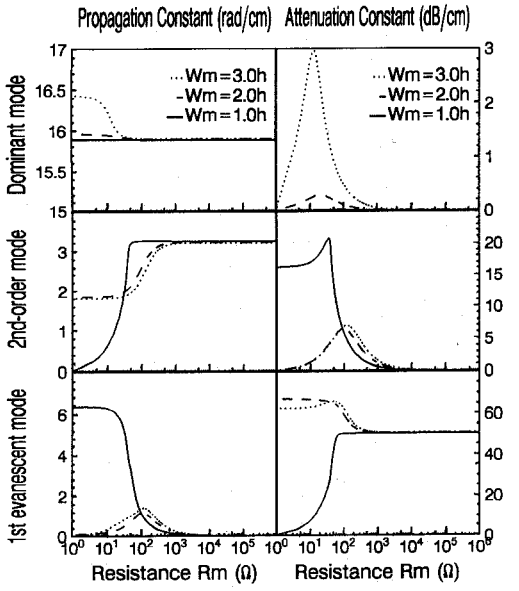

Fig. 3. The propagation constants (left column) and attenuation constants (right column), as functions of the film resistance R_m, for the dominant mode (top row), the second-order mode (middle row), and the first evanescent mode (bottom row). $f = 25$ GHz.

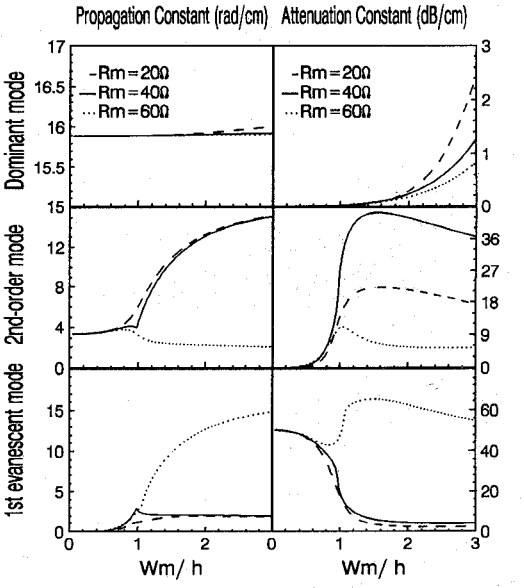

Fig. 4. The propagation constants (left column) and attenuation constants (right column), as functions of the normalized film width W_m/h, for the dominant mode (top row), the second-order mode (middle row), and the first evanescent mode (bottom row). $f = 25$ GHz.

shielded microstrip line, and Fig. 2(b) shows those for the shielded coplanar waveguide. The results obtained from the present analysis (solid lines) are compared with those independently calculated from the spectral domain approach (SDA) (dash lines). It is seen that, for all the modes existing in the frequency range considered, the curves computed from the present study match quite well with those from the SDA. This ensures the correctness of the current work.

In the following the influences of changing the resistance R_m and the width W_m of the resistive film on the modal characteristics of the shielded microstrip line are analyzed. The frequency is fixed at 25 GHz. From Fig. 2(a) it is seen that there are two propagation modes, i.e., the dominant mode and the second-order (propagation) mode, existing at this frequency. Besides, as the film resistance is varied from infinity (microstrip line) to zero (coplanar waveguide), the first evanescent mode of the unloaded shielded microstrip line may turn into a propagation mode for some film widths (as can be seen from Fig. 3). Therefore, the variations of the characteristics of these three modes are emphasized in the next examples.

Fig. 3 displays the changes of the propagation and attenuation constants for the first three modes, as functions of the resistance R_m. The results for three different film widths, i.e., $W_m = 1h$, $2h$, $3h$, are presented for comparison. (Note that the scales of the sub-figures are different.) It is seen from all the sub-figures that the variation of R_m has almost no influence on the modal characteristics until R_m diminishes below 1 k Ω. For the dominant mode (the top sub-figures), the wider the film is, the more the complex propagation constant is affected by the change of R_m. This is obvious because the wider resistive film gets closer to the center strip and thus has larger influence on the dominant mode. It is noticed that the variation of R_m has nearly no effect on the properties of the dominant mode for the structure with $W_m = 1h$. When R_m is changed from infinity to zero, the second-order propagation mode and the evanescent mode (of the microstrip line), respectively, remain a higher-order propagation mode and an evanescent mode (of the coplanar waveguide) for both $W_m = 2h$ and $3h$. But for $W_m = 1h$, the two modes interchange, that is, the propagation mode of the microstrip line changes into an evanescent mode of the coplanar waveguide, and vice versa.

It is observed that for the structures with film widths $2h$ and $3h$, the evanescent mode can be neglected as compared with the second-order mode, since the attenuation constant of the former is far larger than that of the latter throughout the resistance range. The largest attenuation of the second-order mode occurs at about $R_m = 100\ \Omega$, both for $W_m = 2h$ and $3h$, where the attenuation constant is approximately equal to 7 dB/cm. However, this maximum attenuation is surpassed when the film width is altered to be 1 h and the resistance is set below about 100 Ω. The maximum attenuation constant of the second-order mode for $W_m = 1h$ is 20.5 dB/cm and occurs at $R_m = 40\ \Omega$. (Note that the attenuation constant of the evanescent mode for $W_m = 1h$ is 27.6 dB/cm at this resistance.) Although the attenuation constant of the second-order mode remains large (above 16 dB/cm) when R_m decreases from 40 Ω to 0 Ω, that of the evanescent mode monotonously diminishes from 27.6 dB/cm to 0 dB/cm. This reveals that 40 Ω is the optimal resistance to damp both the second-order mode and the evanescent mode (for $W_m = 1h$).

In summary, Fig. 3 tells that the best choice of the three resistive films to damp the higher-order (or parasitic) modes and not to sway the dominant mode is that of $W_m = 1h$ with $R_m = 40\ \Omega$.

In contrast to varying the film resistance while fixing the width, we then investigate the effects of changing the width with fixed resistances. This enables us to find more precise values of the film widths. Fig. 4 shows the results for $R_m = 20\ \Omega$, 40 Ω, and 60 Ω, in which 40 Ω has been predicted in the discussions of Fig. 3 to be the optimal resistance for a film width of $1h$. From the top sub-figures both the propagation and attenuation constants of the dominant mode have negligible change provided the width is kept smaller than 1 h. When the width increases beyond this value, the film begins to interfere with the dominant mode, which results in the monotonous increases of the attenuation constants. The smaller the resistance is, (i.e., the film becomes more close to a perfect electric conductor), the stronger this interference is.

For all the resistances considered, the attenuation constants for the second-order mode first increases and then decreases with the raise of the film width. This is not the case for the evanescent mode. The curves in the bottom-right sub-figure show that the attenuation

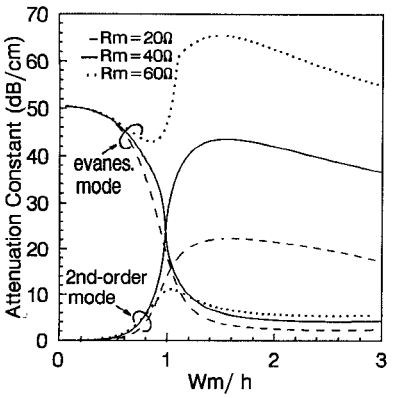

Fig. 5. Attenuation constants, as functions of the normalized film width W_m/h, of the second-order and the first evanescent modes for $R_m = 20$, 40, 60Ω. $f = 25$ GHz.

constants for $R_m = 20\ \Omega$ and 40 Ω continuously decrease with the increase of the width, with a sharp variation around $W_m = 1h$, and that the attenuation for $R_m = 60\ \Omega$ oscillates when the width changes. The different behaviors between the attenuation constant for the second-order mode and that for the evanescent mode suggest that an optimal choice of the film width can be found for each resistance.

The aim for the present analysis is to search for a best design so that the smallest of the losses for the higher-order (parasitic) modes becomes largest. For this we conjoin the curves for the attenuation constants of the two higher-order modes, as shown in Fig. 5. It is seen that the curves of the second-order and evanescent modes for $R_m = 20\ \Omega$ and 40 Ω have cross points. The cross points occur at $W_m = 1.03h$ for $R_m = 20\ \Omega$ and at $W_m = 0.98h$ for $R_m = 40\ \Omega$, with the attenuations being, respectively, 15.7 dB/cm and 23.9 dB/cm. When the film width is chosen different from the width of the cross point, the attenuation constant of one of the two modes becomes less than that of the point. This means that the film width corresponding to the cross point is the best choice to equally suppress both the second-order and the evanescent modes. On the other hand, since the two curves for $R_m = 60\ \Omega$ do not cross each other, the choice for this resistance is the width corresponding to the maximum point of the lower curve (which is, as observed from the figure, that of the second-order mode). The attenuation constant for this maximum point is 11 dB/cm. After putting these together and comparing the attenuation values of the choices for the three resistances considered, it is obvious that the film with a resistance of 40 Ω and a width of $0.98h$ is the optimal selection. To ensure that there are no other higher-order modes whose attenuation constants are smaller than 23.9 dB/cm under this selection, we have plotted the contour lines of $|\det\{\mathbf{Z}^{\mathbf{m}}(\gamma)\}|$ on the complex γ plane (not shown here). The result shows that, in the range of $0 \leq \beta \leq 16$ (rad/cm) and $0 \leq \alpha \leq 40$ (dB/cm), where β and α are the propagation and attenuation constants, only three zeros of the determinant can be found, which exactly correspond to those of the dominant mode ($\beta = 15.9$ rad/cm, $\alpha = 0$ dB/cm), the second-order mode (β =3.8 rad/cm, $\alpha = 23.9$ dB/cm), and the first evanescent mode ($\beta = 3.0$ rad/cm, $\alpha = 23.9$ dB/cm).

IV. Conclusion

In this paper, the suppression of the higher-order parasitic modes of a shielded microstrip line has been analyzed by coating resistive films on the two sides of the center strip. The analysis is based on the use of the method of lines with some modification concerning the inhomogeneity of the surface between the air and the substrate layer. The resistance and the width of the film have been varied to see the influence on the suppression effects to the modes of a microstrip with housing 10 $h\times$ 7 h. It is found that, provided the resistance is larger than 1 kΩ, and the width is less than $3h$, the resistive film nearly has no effect on the three modes. Also, there exists an optimal combination of the film width and resistance so that the resistive film has the largest attenuating effect on the higher-order modes but has no interference with the dominant mode. The optimal width is 0.98 h and the corresponding resistance is 40 Ω. The attenuation of the higher-order modes under this combination is found to be 23.9 dB/cm.

References

[1] L. P. Dunleavy and P. B. Katehi, "Shielding effects in microstrip discontinuities," *IEEE Trans. Microwave Theory Tech.*, vol. 36, pp. 1767–1774, Dec. 1988.

[2] R. H. Jansen and L. Wiemer, "Full wave theory based development of MM-wave circuit models for microstrip open end, gap, step, bend and tee," in *IEEE MTT-S Int. Microwave Symp. Dig.*, 1989, pp. 779–782.

[3] R. K. Hoffmann, *Handbook of Microwave Integrated Circuits*. Norwood, MA: Artech House, 1987, pp. 399–400.

[4] A. F. Armstrong and P. D. Cooper, "Techniques for investigating spurious propagation in enclosed microstrip," *The Radio and Electronic Engineer.*, vol. 48, no. 1/2, pp. 64–72, Jan./Feb. 1978.

[5] M. V. Schneider and B. S. Glance, "Suppression of waveguide modes in strip transmission lines," *Proc. IEEE*, p. 1184, Aug. 1974.

[6] D. F. Williams, "Damping of the resonant modes of a rectangular metal package," *IEEE Trans. Microwave Theory Tech.*, vol. 37, pp. 253–256, Jan. 1989.

[7] John J. Burke and Robert W. Jackson, "Reduction of parasitic coupling in packaged MMIC's," in *IEEE MTT-S Int. Microwave Symp. Dig.*, 1990, pp. 255–258.

[8] S. J. Chung and L. K. Wu, "Analysis of the effects of a resistively coated upper dielectric layer on the propagation characteristics of hybrid modes in a waveguide shielded microstrip using method of lines," *IEEE Trans. Microwave Theory Tech.*, vol. 41, pp. 1393–1399, Aug. 1993.

[9] T. B. A. Senior, "Approximate boundary condition," *IEEE Trans. Antennas Propagat.*, vol. AP-29, pp. 826–829, Sept. 1981.

[10] R. Pregla and W. Pascher, "The method of lines," in *Numerical Techniques for Microwave and Millimeter-Wave Passive Structures*, T. Itoh, Ed. New York: Wiley, 1989, ch. 6.